JOURNAL OF SPACECRAFT AND ROCKETS
Vol. 31, No. 4, July–August 1994

# Engineering Notes

*ENGINEERING NOTES are short manuscripts describing new developments or important results of a preliminary nature. These Notes cannot exceed 6 manuscript pages and 3 figures; a page of text may be substituted for a figure and vice versa. After informal review by the editors, they may be published within a few months of the date of receipt. Style requirements are the same as for regular contributions (see inside back cover).*

## Effects of Space Exposure on Pyroelectric Infrared Detectors

James B. Robertson*
*NASA Langley Research Center,*
*Hampton, Virginia 23681*

### Nomenclature

$A_d$ = detector area, $cm^2$
$H$ = radiant energy flux, $W/cm^2$
$N$ = noise, rms V
$S$ = signal, rms V
$\Delta f$ = bandwidth, Hz

### Introduction

NASA's commitment to air-pollution monitoring and thermal mapping of the Earth requires photodetection in the 6–20 μ region of the spectrum. Photovoltaic detectors must be cooled to detect radiation at these wavelengths, and the cryogenic systems required are large, complex, and expensive. Pryoelectric detectors can detect in the 1–100 μ region while operating at room temperature, making them candidates for NASA's infrared detector requirements. The effects of launch and space exposure on the performance of pyroelectrics must be determined before they can be used with confidence in space.

This study of long-term space exposure on pyroelectric detectors was one of fifty-seven experiments which flew onboard a spacecraft known as the long duration exposure facility or LDEF.[1] The LDEF was placed into a 257-mile-high orbit on April 6, 1984 and was retrieved on January 12, 1990. At the time of retrieval, the LDEF's orbit had decayed to an altitude of 179 miles.

The objective of this experiment was to determine the effects of launch and long-term space exposure on a selection of the most widely used pyroelectric detectors available at the time of the experiment. The experimental approach was to measure performance parameters of the detectors before and after flight on the LDEF and determine changes in detector performance.

### Experiment

Twenty pyroelectric detectors were flown on the LDEF and another nine were stored in unsealed containers on the ground as control samples. The detectors were mounted on tray E-5 of the LDEF. Tray E-5 was located on the trailing side (the side of the LDEF facing away from the direction of orbital flight). Experiments on the trailing side experienced solar radiation, space radiation, and meteoroid impacts but were spared the ram effects experienced by the leading side, e.g., collisions with upper-atmospheric gas molecules and space debris. The tray was covered with a perforated aluminum plate for thermal control. The plate blocked 50% of incident radiation. Four of the 20 flight detectors were further covered with a solid aluminum plate which shielded them from space radiation but left them exposed to space vacuum.

The detectors used in the experiment comprised three different pyroelectric materials and three different window materials shown in Fig. 1. The detector materials included lithium tantalate (LT), strontium barium niobate (SBN), and triglycine sulfate (TGS). Some of the detector housings had infrared-transmitting materials in their windows, and some did not. The window materials included zinc sulfide (ZnS), thalium bromide iodide (T1BrI, a.k.a. KRS-5), and polished germanium (Ge).

The primary figure of merit for infrared detectors is the detectivity, $D^*$. $D^*$ is calculated from the measured values of signal and noise voltage using the following equation:

$$D^* = \frac{S/N\sqrt{\Delta f}}{H\sqrt{A_d}} \qquad \left(\frac{cm\sqrt{Hz}}{W}\right) \tag{1}$$

Signal and noise measurements were made using a 500-K blackbody radiation source, a light chopper, a preamplifier, and a wave analyzer. The measurements were made at chopping frequencies of 5, 10, 20, and 50 Hz.

### Results

The results of the postflight detectivity measurements are summarized in Table 1. The table lists the detectors according to detector material, window material, and location of the detector during the experiment (i.e., control sample, exposed flight sample, or flight sample covered by the aluminum plate). Changes in noise measurement less than +/− 25% are not considered statistically significant.

Among the LT detectors there were three failures, i.e., no signal or erratic, unrepeatable signal. Erratic output signals suggest mechanical failure rather than radiation damage to pyroelectric material. The failure rate among the flight LT detectors (two out of nine) was comparable to that for the control LT detectors (one out of four). Differences between the preflight and postflight detectivities were within the error bounds of the measurement with one exception. The exception was an LT detector with a T1BrI window whose postflight signal was 38% less than its preflight signal. This loss is attributed to a decrease in transmissivity of the window material which is discussed in a later paragraph. This decrease in signal combined with a 57% increase in noise produced a 61% decrease in $D^*$.

All of the SBN detectors survived the storage and flight. Differences between postflight and preflight detectivities were all within the bounds of measurement repeatability.

The detectors made of TGS did not fare well, either during flight or storage. Three of the four TGS flight detectors had zero signal response after flight. The fourth flight detector maintained its signal strength but had a 40% increase in noise. All of the TGS control detectors (four out of four) suffered a complete loss of signal during storage on the ground. The failure of the TGS detectors during flight cannot be ascribed to space exposure since all of the control detectors failed during the same period of time.

Received May 27, 1993; revision received Aug. 2, 1993; accepted for publication Aug. 3, 1993. 

*Aerospace Technologist.

**Table 1 Changes in detector parameters**

| Detector type (no. of samples) | Window material | Location during flight | % change signal (avg.) | % change noise (avg.) | % change $D^*$ (avg.) |
|---|---|---|---|---|---|
| LT (1) | None | Control | + 2.5 | − 9 | + 5.8 |
| LT (1) | None | Control | Failed | | |
| LT (1) | None | Covered | + 1.0 | − 10 | + 5 |
| LT (1) | None | Exposed | Erratic | | |
| LT (3) | None | Exposed | − 5.3 | + 1 | − 10 |
| LT (2) | ZnS | Control | − 4.0 | + 23 | − 23 |
| LT (1) | ZnS | Covered | −3.5 | + 4 | − 5.5 |
| LT (1) | ZnS | Exposed | Erratic | | |
| LT (3) | ZnS | Exposed | − 6.7 | + 24 | − 25 |
| LT (1) | TlBrI | Exposed | − 38 | + 57 | − 61 |
| SBN (1) | Ge | Control | + 0.5 | + 1 | 0 |
| SBN (1) | Ge | Covered | − 1.4 | + 1 | + 2 |
| SBN (4) | Ge | Exposed | − 2.0 | − 22 | + 28 |
| TGS (4) | TlBrI | Control | Failed | | |
| TGS (1) | TlBrI | Covered | Failed | | |
| TGS (2) | TlBrI | Exposed | Failed | | |
| TGS (1) | Ge | Exposed | 0 | + 40 | − 30 |

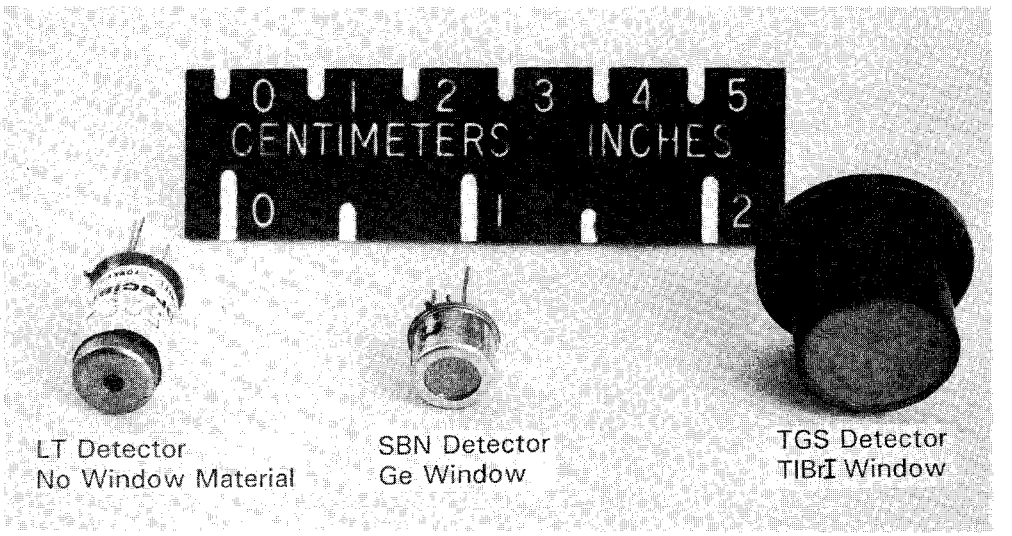


**Fig. 1 Three pyroelectric detector types.**

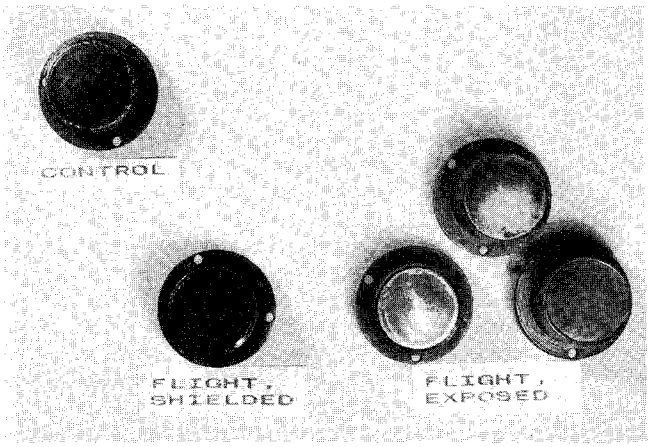


**Fig. 2 Postflight photo of detectors showing damage to TlBrI windows.**

There was no visible damage in either the Ge or ZnS windows. Also, there was no significant loss in signal strength of the flight detectors having these window materials.

The TlBrI windows which were exposed during flight sustained noticeable damage. The damage was in the form of nonuniform white areas on the front surface of the windows, shown in Fig. 2. This effect was not present in the TlBrI windows of the covered flight detector or in the control detectors. Transmission measurements were made on two of the damaged TlBrI windows and on a TlBrI window from one of the control detectors. Loss of transmission through the damaged windows ranged from 17% to 50% depending upon the window and the location on each window; greater transmission loss corresponded to regions of greater visible damage. Only one detector containing a TlBrI window was operable after flight. This detector was made of lithium tantalate. The decrease in signal strength from this detector after flight was 38%. This is consistent with the amount of IR transmission loss in the damaged TlBrI windows. All of the other TlBrI-windowed detectors were made of TGS.

Electron spectroscopy for chemical analysis (ESCA) was performed on the damaged TlBrI windows. The analysis showed the presence of silicon, in the form of silicates, on the surface of the exposed windows. The Si concentration was higher in the regions of lesser damage and lower in regions of greater damage. Another significant result of the analysis was the change in the ratio of thalium to bromine, Tl:Br, in the surface of the exposed windows. In the control window, the Tl:Br ratio is approximately 1:1. In the low-damage areas of the exposed windows the Tl:Br ratio was 4.6:1, and in the high-damage areas the Tl:Br ratio was >26:1 (see Table 2).

**Table 2 ESCA analysis of TlBrI windows**

| Sample | Si concentration, atomic % | Tl:Br ratio |
|---|---|---|
| Control | 0 | 1:1 |
| Exposed, min. damage[a] | 17 | 5:1 |
| Exposed, max. damage[b] | 6 | >26:1 |

[a]Areas of lesser clouding and lesser loss of transmissivity.
[b]Areas of greater clouding and greater loss of transmissivity.

## Conclusions

This experiment has shown that pyroelectric detectors made of lithium tantalate or strontium barium niobate are suitable for long-term space use. The LT and SBN detectors survived six years of storage plus almost six years of exposure to space with little or no loss of performance. The detectors made of TGS cannot be recommended because of their apparently short shelf life. Seven of the eight TGS detectors failed to respond after storage and/or flight.

The TlBrI windows experienced noticeable damage. The damage was not uniform and was limited to the detector windows that had direct exposure to space. The inverse relationship between the concentration of silicon on the window surface and the amount of bromine lost suggests that the silicate acted as a shield which lessened the loss of bromine and iodine. Since there was no damage to either the ZnS or the Ge windows, these materials can be recommended as window or lens material for long-term use in space.

This experiment shows that the choice of window and lens materials are of major importance. When used in space, a detector will be part of a system and will be located behind a lens or window of some sort. Damage to the lens or windows will most likely play a larger role in loss of system performance than will damage to the detector material.

## References

[1] O'Neal, R. L., and Lightner, E. B., "Long Duration Exposure Facility—A General Overview," *LDEF—69 Months in Space, First Post-Retrieval Symposium*, NASA CP-3134, Part 1, June 1991, pp. 3–48.

Ronald K. Clark
*Associate Editor*

# Mars Aerocapture: Extension and Refinement

P. F. Wercinski*
*NASA Ames Research Center, Moffett Field, California 94035*
and
J. E. Lyne†
*University of Tennessee, Knoxville, Tennessee 37996*

## Nomenclature

$A$ = vehicle reference area for aerodynamic coefficients, m$^2$
$C_D$ = drag coefficient
$D$ = drag, N
$L$ = lift, N
$L/D$ = lift over drag
$m$ = vehicle mass, kg
$V_e$ = atmosphere entry velocity, km/s
$\Delta V$ = velocity change, km/s
$\beta$ = ballistic coefficient, kg/m$^2$

Received March 24, 1993; accepted for publication March 24, 1993.

*Aerospace Engineer, Thermosciences Division. Member AIAA.
†Assistant Professor, Deptartment of Mechanical and Aerospace Engineering. Member AIAA.

## Introduction

SPACE missions that use the Martian atmosphere for decelerating both manned and unmanned spacecraft arriving along hyperbolic trajectories have been studied for decades. Previous studies,[1-4] as well as a more recent one by Lyne[5] have shown the effects of varying mission design parameters such as ballistic coefficient ($m/C_DA$), entry velocity ($V_e$), lift over drag ($L/D$), and deceleration limits on the selection of entry vehicle shapes and thermal protection systems. This note is intended to extend and revise previous aerocapture parametric studies for both low-energy (500-km circular) orbits and for high-energy (1-sol period, 500-km periapsis) orbits at Mars.

Specifying the atmosphere entry velocity for a desired vehicle configuration, i.e., $L/D$ and $\beta$, will determine the allowable entry corridor for a vehicle aerocapturing at Mars. The entry corridor is defined as the range of atmospheric entry angles determined by the limiting conditions of undershoot and overshoot that will permit capture to a desired parking orbit as shown in Fig. 1. The overshoot trajectories are the shallowest entries that assure atmospheric capture with the vehicle entering in a lift-down attitude. Undershoot trajectories are flown in a lift-up attitude and are constrained either by $g$-loading or peak heating rates. The difference between the overshoot and undershoot trajectory entry flight path angles defines the entry corridor width.

## Discussion

Recent manned Mars mission design studies[6] have proposed conjunction-class interplanetary trajectory missions that would

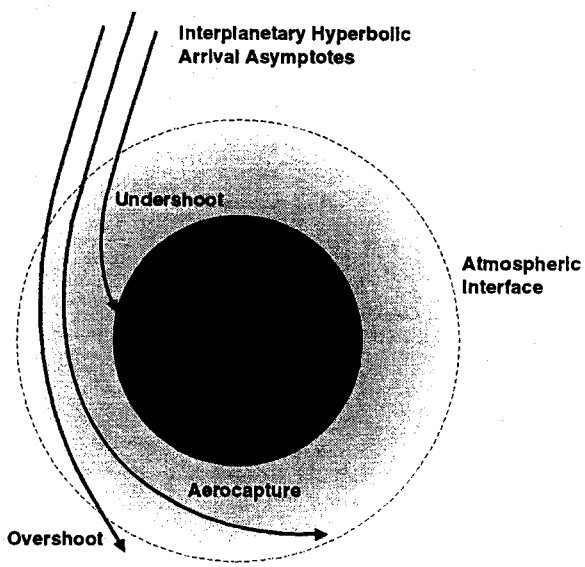


**Fig. 1 Aerocapture at Mars.**